ISSN 1063-7710, Acoustical Physics, 2014, Vol. 60, No. 4, pp. 492–498. © Pleiades Publishing, Ltd., 2014.

PHYSICAL FOUNDATIONS OF ENGINEERING ACOUSTICS

# A Study of Stepped Acoustic Resonator with Transfer Matrix Method[1]

**Qi Min, Wan-Quan He, Quan-Biao Wang, Jia-Jin Tian, and Qing-You Zhang**

*Department of Physics, Honghe University, Mengzi, Yunnan, 661100 P.R. China*

*e-mail: minq7@163.com*

Received December 23, 2013

**Abstract**—Transfer matrix method was applied in the study of stepped acoustic resonators. Transfer matrix method was more competent in comparison with analytic method to investigate the acoustic properties of stepped acoustic resonator, especially multi-step acoustic resonator. With the help of the numerical solution, the resonance frequencies, the phase angles and the radiation impedances of stepped acoustic resonators which consisted of one to five sub-tubes were studied theoretically and experimentally. The numerical solutions were in excellent agreement with the experimental results.

*Keywords*: stepped acoustic resonator, transfer matrix method, nonequidistant spectrum, phase angle, radiation impedance.

**DOI:** 10.1134/S1063771014040095

## 1. INTRODUCTION

In general, people use a tube closed at its two ends as an acoustic resonator or standing-wave tube [1, 2]. This kind of resonator has an equidistant resonance frequency spectrum in which harmonics of fundamental resonance frequency coincide with higher order resonance frequencies [3, 4]. Unlike that, there is other kind of acoustic resonator which consists of two or more sub-tubes of different radiuses as shown in Fig. 1. With the geometric construction, the latter kind of resonator has a nonequidistant spectrum, i.e., the higher resonance frequencies are not the integer multiples of the fundamental resonance frequency [4–7]. Gaitan and Atchley called the former kind of acoustic resonator as "harmonic" resonator and Y.A. Ilinskii et al. called it "consonant" resonator, while, for the latter kind of resonator, Gaitan and Atchley named it as "anharmonic" resonator and Ilinskii et al. named it "dissonant" resonator [8, 9]. Moreover, Denardo and Alkov referred to the latter kind of resonator as having "nonuniformity" [10, 11]. Here, we called the latter kind of acoustic resonator as stepped acoustic resonator.

Stepped acoustic resonators are very interesting apparatus in acoustic field. For example, people could use them to obtain and study high-amplitude standing wave in nonlinear acoustics [1, 4–7]. Gibiat et al. presented a theoretical and experimental investigation for acoustic multiscattering in a stepped acoustic resonator with a Cantor-like structure. Homothetic acoustical features and forbidden bands as well as wave trapping phenomena were reported [12]. Because the apparatus has a simple piecewise-uniform acoustic unit sub-tube that can easily be changed, alterations of the nonuniformity in cross-sectional area were utilized to change the resonance frequency and to yield two, three, or four frequencies whose differences correspond to musical intervals. The effect of nonuniformity on acoustic waves as educational demonstration has been fully displayed by Denardo and Bernard [10, 11].

On solving resonance frequencies of two-step resonator, Denardo and Bernard gave three different analytic methods: imposing boundary conditions on solutions of wave equation, the energy method of Rayleigh, and the theorem of adiabatic invariance. The solution procedure was somewhat complex, however. Furthermore, to solve analytically resonance frequency would become more and more difficult as the number of sub-tube increases, let alone the other acoustic quantities such as phase angle and radiation impedance [8, 10, 11].

Transfer matrix method was first applied by Stewart and Lindsay to acoustic filter design in 1930 [13, 14]. This method was also called two-port or four-pole method, and meanwhile, the transfer matrix was

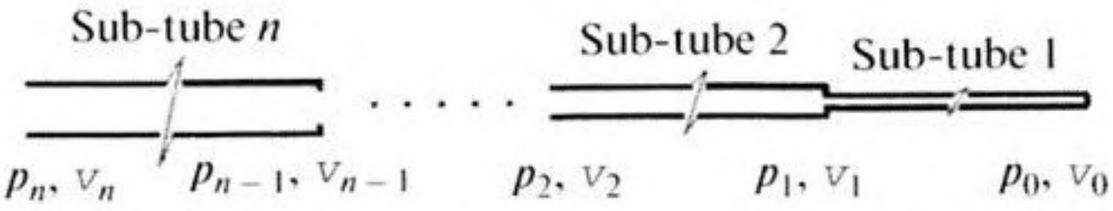


**Fig. 1.** Geometry of the $n$-step resonator.

[1] The article is published in the original.

called transmission matrix or four-pole parameter representation. Transfer matrix method has most often been applied to the characterization of duct system component, exhaust silencer, etc. Transfer matrix method could also be applied as an adjunct to boundary element method or finite element method in noise-control design procedures.

With transfer matrix method, it was convenient to model an acoustic apparatus which consists of one or more acoustic units. Each acoustic unit can be simply regarded as a "black box" with two ports, one is input port and the other—output port [15, 16]. Any individual transfer matrix presenting each acoustic unit is derived by solving a constant-coefficient acoustic state variable differential equation. As for the whole acoustic matrix of an acoustic apparatus of more than one acoustic unit, apart from individual transfer matrices, there is a connection matrix between every two adjacent individual transfer matrices. The whole transfer matrix for the overall acoustic apparatus is then obtained by multiplying in turn the individual transfer matrices and the connection matrices. As a result, acoustic analysis of such an apparatus could be greatly simplified with the transfer matrix method.

Taking air as working medium, in this paper we used the transfer matrix method to investigate acoustic properties of stepped acoustic resonators which consist of one to five sub-tubes at room temperature. With the help of transfer matrix, the resonance frequency, the phase angle and the radiation impedance were studied theoretically and experimentally. The method can be extended to any other multi-step acoustic resonator.

## 2. TRANSFER MATRIX METHOD

The geometry of the $n$th sub-tube of the stepped resonator is shown in Fig. 2, and its equivalent circuit is shown in Fig. 3. As shown in Fig. 2, $l_n$ is the length of the $n$th sub-tube and $d_n$ is the diameter. In Fig. 3, $Y_n = \rho_0 c_0$ is the acoustic characteristic impedance, where $\rho_0$ is the air density and $c_0$ is the sound speed in air. The individual transfer matrix of the $n$th sub-tube is a 1D matrix $[T_n]$, a $2 \times 2$ transfer matrix, which connects the sound pressure $p_n$ and the normal acoustic particle velocity $v_n$ on the input port with those, $p_{n-1}$ and $v_{n-1}$, on the out port of the $(n-1)$th sub-tube, i.e.,

$$\begin{bmatrix} p_n \\ v_n \end{bmatrix} = \begin{bmatrix} T_{11}(n) & T_{12}(n) \\ T_{21}(n) & T_{22}(n) \end{bmatrix} \begin{bmatrix} p_{n-1} \\ v_{n-1} \end{bmatrix}, \quad n = 1, 2, 3.... \quad (1)$$

It is then of interest to determine the four elements of the individual transfer matrix $|T_n|$. As shown in Eq. (1), the acoustic variables at one port can be determined by the plane wave components at the other port if the individual transfer matrix $|T_n|$ is known, since the elements of the individual transfer matrix $|T_n|$ directly relate the acoustic variables of the two ports.

Taking $p_{Ai}$ as the sound pressure amplitude of positive-going plane wave and $p_{Ar}$ as that of negative-going plane wave, meanwhile $\alpha_n = 6.36 \times 20^{-4}\sqrt{f/d_n}$ as the attenuation coefficient [1], one may express the pressure and the particle velocity in the $n$th sub-tube in terms of the positive- and negative-going plane wave components, i.e.,

$$\begin{cases} p(x) = p_{Ai} e^{-\alpha_n x} e^{j(\omega t - kx)} + p_{Ar} e^{\alpha_n x} e^{j(\omega t + kx)}, \\ v(x) = v_{Ai} e^{-\alpha_n x} e^{j(\omega t - kx)} + v_{Ar} e^{\alpha_n x} e^{j(\omega t + kx)}. \end{cases} \quad (2)$$

Thus, the pressures and the particle velocities on the input and output ports have the following relationship:

$$\begin{aligned} p_n = p_{Ai} + p_{Ar} &= \frac{1}{2} Y_n \left[ \left( v_{n-1} - \frac{p_{n-1}}{Y_n} \right) e^{jkl_n} e^{\alpha_n l_n} \right. \\ &\left. - \left( v_{n-1} + \frac{p_{n-1}}{Y_n} \right) e^{-jkl_n} e^{-\alpha_n l_n} \right] \quad (3a) \\ &= \frac{1}{2} [ v_{n-1} Y_n (e^{jkl_n} e^{\alpha_n l_n} - e^{-jkl_n} e^{-\alpha_n l_n}) \\ &- p_{n-1} (e^{jkl_n} e^{\alpha_n l_n} + e^{-jkl_n} e^{-\alpha_n l_n}) ], \end{aligned}$$

$$\begin{aligned} v_n = v_{Ai} + v_{Ar} &= \frac{1}{2} \left[ \left( v_{n-1} - \frac{p_{n-1}}{Y_n} \right) e^{jkl_n} e^{\alpha_n l_n} \right. \\ &\left. + \left( v_{n-1} + \frac{p_{n-1}}{Y_n} \right) e^{-jkl_n} e^{-\alpha_n l_n} \right] \quad (3b) \\ &= \frac{1}{2} [ v_{n-1} (e^{jkl_n} e^{\alpha_n l_n} + e^{-jkl_n} e^{-\alpha_n l_n}) \\ &- \frac{p_{n-1}}{Y_n} (e^{jkl_n} e^{\alpha_n l_n} - e^{-jkl_n} e^{-\alpha_n l_n}) ]. \end{aligned}$$

The acoustic variables of the two ports can be linked as

$$\begin{bmatrix} p_n \\ v_n \end{bmatrix} = \begin{bmatrix} \frac{1}{2}(e^{jkl_n} e^{\alpha_n l_n} + e^{-jkl_n} e^{-\alpha_n l_n}) & \frac{Y_n}{2}(e^{jkl_n} e^{\alpha_n l_n} - e^{-jkl_n} e^{-\alpha_n l_n}) \\ \frac{1}{2Y_n}(e^{jkl_n} e^{\alpha_n l_n} - e^{-jkl_n} e^{-\alpha_n l_n}) & \frac{1}{2}(e^{jkl_n} e^{\alpha_n l_n} + e^{-jkl_n} e^{-\alpha_n l_n}) \end{bmatrix} \begin{bmatrix} p_{n-1} \\ v_{n-1} \end{bmatrix}. \quad (4)$$

Obviously, the individual transfer matrix $[T_n]$ is

$$[T(n)] = \begin{bmatrix} \frac{1}{2}(e^{jkl_n}e^{\alpha_n l_n} + e^{-jkl_n}e^{-\alpha_n l_n}) & \frac{Y_n}{2}(e^{jkl_n}e^{\alpha_n l_n} - e^{-jkl_n}e^{-\alpha_n l_n}) \\ \frac{1}{2Y_n}(e^{jkl_n}e^{\alpha_n l_n} - e^{-jkl_n}e^{-\alpha_n l_n}) & \frac{1}{2}(e^{jkl_n}e^{\alpha_n l_n} + e^{-jkl_n}e^{-\alpha_n l_n}) \end{bmatrix}. \quad (5)$$

One may note $T_{11}(n) = T_{22}(n)$ in the individual transfer matrix $[T_n]$. This results from the constraints placed on the individual transfer matrix elements by the requirements of symmetry when the acoustical unit is reciprocal. For the $n$-step resonator, the connection matrix $[S_n]$ is also a $2 \times 2$ transfer matrix [17]. The overall transfer matrix then is

$$\begin{bmatrix} p_n \\ V_n \end{bmatrix} = [T_n]\begin{bmatrix} 1 & 0 \\ 0 & s_n \end{bmatrix}[T_{n-1}]\begin{bmatrix} 1 & 0 \\ 0 & s_{n-1} \end{bmatrix}\cdots[T_1]\begin{bmatrix} p_0 \\ V_0 \end{bmatrix}, \quad (6)$$

where $s_n = d_n^2/d_{n-1}^2$ that makes for the connection matrix $[S_n]$ represents the Kirchhoff conditions at the diameter discontinuity between the $n$th and the $(n-1)$th sub-tubes. By imposing port conditions, the acoustic properties of the stepped resonator can be obtained from the equations on the elements of the overall transfer matrix. These equations usually can only be solved numerically because they are transcendental about the angular frequency $\omega$. Compared with analytic method, when the number of the sub-tubes increases, transfer matrix method would become increasingly convenient with the help of numerical solution.

## 3. EXPERIMENTAL SETUP

The experimental setup consists of three parts as shown in Fig. 4, namely the stepped resonator, the signal driver, and the signal processing system.

### *3.1. The Stepped Resonator*

All sub-tubes of the stepped resonators are made of stainless steel and are connected with stainless steel stepping ring. The two ports of all the stepped resonators are capped by stainless steel caps. In the center of each cap, there is a micropore of 7 mm to install microphone. The thickness of all rings, caps and sub-tubes exceed 10 mm so that the whole stepped resonator is heavy enough to overcome the influence of vibration induced by loudspeaker. There are five different types of tube employed as the sub-tube in the present paper. The dimensions of them are listed in table. For comparison, the lengths of all tubes are approximately equal to 1000 mm.

### *3.2. The Signal Driver*

The loudspeaker McCauley 2010 used here is made in America and whose caliber is 10 ft and resistance 8 Ω. Through a horny stepping ring, the loudspeaker is connected to the hole at the input port of stepped resonator. The loudspeaker is driven by the amplifier DSA1850B also made in America and the drive signal is sent by the control block 7540 of B&K Pulse3560C.

### *3.3. The Signal Processing System*

The signals of sound pressure at both ports of the stepped resonator are acquired by the microphones installed in the pores of the two port caps. Both of the microphones are electret microphone BK4944 whose sensitivity and measuring range are 1.0 mV/Pa and 46–170 dB respectively. The signals gathered by two microphones are real-time processed by the control block of the B&K Pulse3560C.

The experiment was operated at ambient atmospheric pressure and real-time monitored by a PC linked to the B&K Pulse3560C.

## 4. RESULTS

### *4.1. One-Step Acoustic Resonator*

Among all stepped acoustic resonators, the one-step resonator has the simplest construction. Its transfer matrix is the base of those of the following kinds of stepped resonators. According to Eqs. (4) and (5), the acoustic variables of the two ports of one-step resonator have the relation

$$\begin{bmatrix} p_1 \\ V_1 \end{bmatrix} = \begin{bmatrix} \frac{1}{2}(e^{jkl_1}e^{\alpha_1 l_1} + e^{-jkl_1}e^{-\alpha_1 l_1}) & \frac{\rho_0 c_0}{2}(e^{jkl_1}e^{\alpha_1 l_1} - e^{-jkl_1}e^{-\alpha_1 l_1}) \\ \frac{1}{2\rho_0 c_0}(e^{jkl_1}e^{\alpha_1 l_1} - e^{-jkl_1}e^{-\alpha_1 l_1}) & \frac{1}{2}(e^{jkl_1}e^{\alpha_1 l_1} + e^{-jkl_1}e^{-\alpha_1 l_1}) \end{bmatrix}\begin{bmatrix} p_0 \\ V_0 \end{bmatrix}. \quad (7)$$

Here and next, there is a boundary condition that the particle velocity $v_0 = 0$ since the output ports of all stepped resonators are sealed off rigidly [18].

With Eq. (7), the numerical solutions of resonance frequency, phase angle and radiation impedance were shown in Fig. 5. Meanwhile, the experimental results of resonance frequency and phase angle were also shown. The numerical solutions are in good agreement with the experimental results. The resonance frequencies, the peaks and the valleys of SPTF (sound pressure transfer function), distribute evenly in frequency domain and all the valleys approach zero. That means the one-step resonator has an equidistant resonance frequency spectrum. The peaks correspond to the fact that the length of one-step resonator is equal to the odd times of half-wavelength while the valleys correspond to the even multiples of half-wavelength.

The phase angle is the relative phase angle between the sound pressures of the input and the output port, which are $p_1$ and $p_0$, respectively, here. The absolute values of phase angle of the peak resonance frequencies are about 90° while those of the valley resonance frequencies are about 0° or 180°. The radiation impedance is that of the input port, namely $p_1/v_1$. The radiation impedance of the first valley resonance frequency is maximum, which exceeds $4 \times 10^4$ kg/cm$^2$, then the radiation impedances of the other valley resonance frequencies decrease in sequence although the SPTF of all the valley resonance frequencies are almost the same. By contrast, the radiation impedances of the peak resonance frequencies are very low and almost approach zero, but now the peaks of resonance frequencies decrease one after another and the maximum exceeds 40 dB at the first peak.

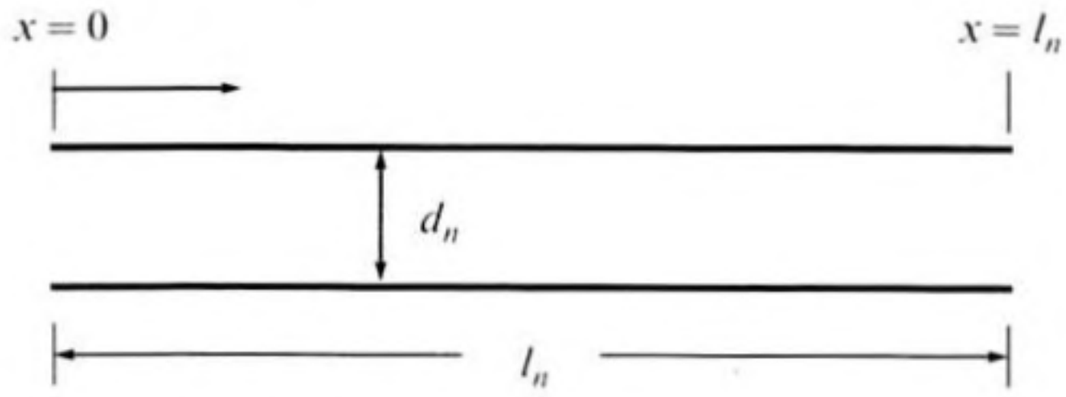


**Fig. 2.** Geometry of the $n$th sub-tube.

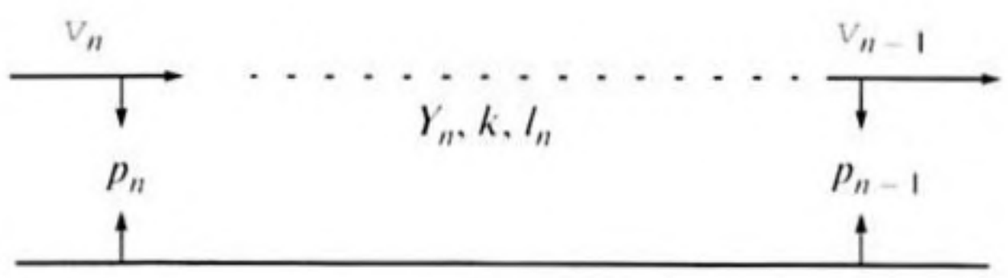


**Fig. 3.** Equivalent circuit of the $n$th sub-tube.

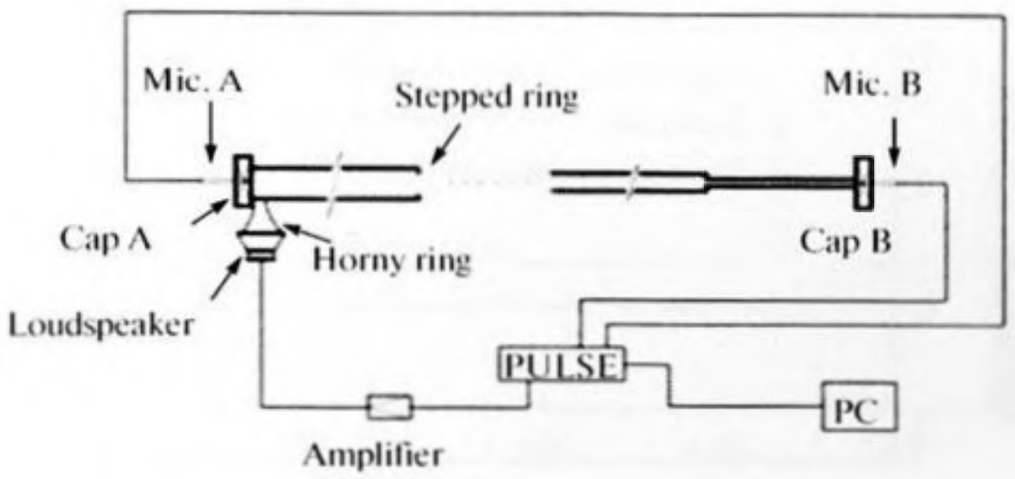


**Fig. 4.** Schematic of experimental setup.

### *4.2. Two-Step Acoustic Resonator*

The acoustic properties, especially the dissonant properties, of a two-step acoustic resonator have been studied by our team [4, 7]. By optimizing the two-step acoustic resonator, with its dissonant properties, a 184 dB extremely nonlinear pure standing-wave field has been obtained at the first resonance frequency. The transfer matrix of two-step resonator is the bridge through which the transfer matrix can evolve from one-step resonator to multi-step ones. Following Eqs. (6) and (7), the acoustic variables of the two ports of a two-step acoustic resonator can be linked as

$$\begin{bmatrix} p_2 \\ v_2 \end{bmatrix} = \begin{bmatrix} \frac{1}{2}(e^{jkl_2}e^{\alpha_2 l_2} + e^{-jkl_2}e^{-\alpha_2 l_2}) & \frac{1}{2}\rho_0 c_0(e^{jkl_2}e^{\alpha_2 l_2} - e^{-jkl_2}e^{-\alpha_2 l_2}) \\ \frac{1}{2}\frac{1}{\rho_0 c_0}(e^{jkl_2}e^{\alpha_2 l_2} - e^{-jkl_2}e^{-\alpha_2 l_2}) & \frac{1}{2}(e^{jkl_2}e^{\alpha_2 l_2} + e^{-jkl_2}e^{-\alpha_2 l_2}) \end{bmatrix}$$
$$\times \begin{bmatrix} \frac{1}{2}(e^{jkl_1}e^{\alpha_1 l_1} + e^{-jkl_1}e^{-\alpha_1 l_1}) & \frac{1}{2}\rho_0 c_0(e^{jkl_1}e^{\alpha_1 l_1} - e^{-jkl_1}e^{-\alpha_1 l_1}) \\ \frac{1}{2}\frac{1}{\rho_0 c_0}\frac{d_1^2}{d_2^2}(e^{jkl_1}e^{\alpha_1 l_1} - e^{-jkl_1}e^{-\alpha_1 l_1}) & \frac{1}{2}\frac{d_1^2}{d_2^2}(e^{jkl_1}e^{\alpha_1 l_1} + e^{-jkl_1}e^{-\alpha_1 l_1}) \end{bmatrix} \begin{bmatrix} p_0 \\ v_0 \end{bmatrix}. \quad (8)$$

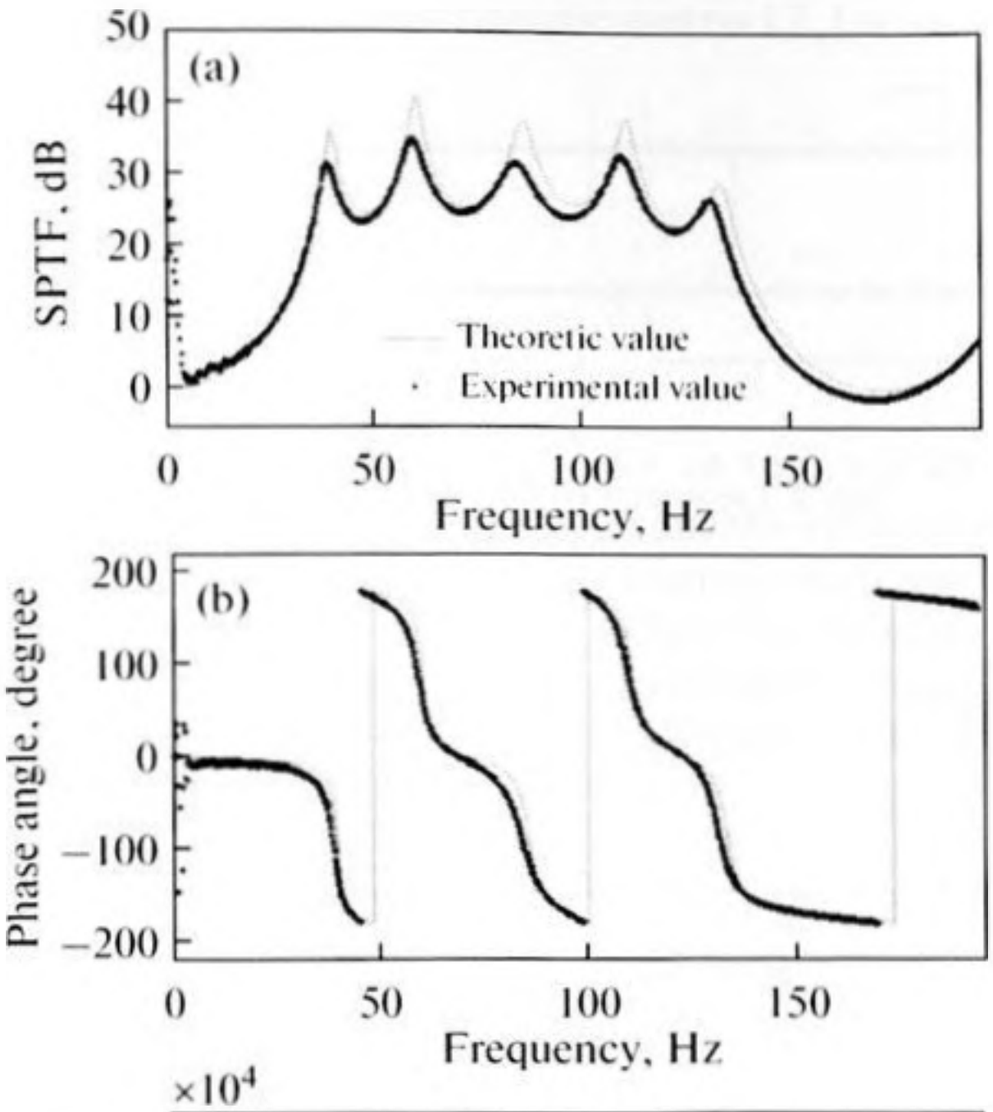


**Fig. 5.** One-step resonator.

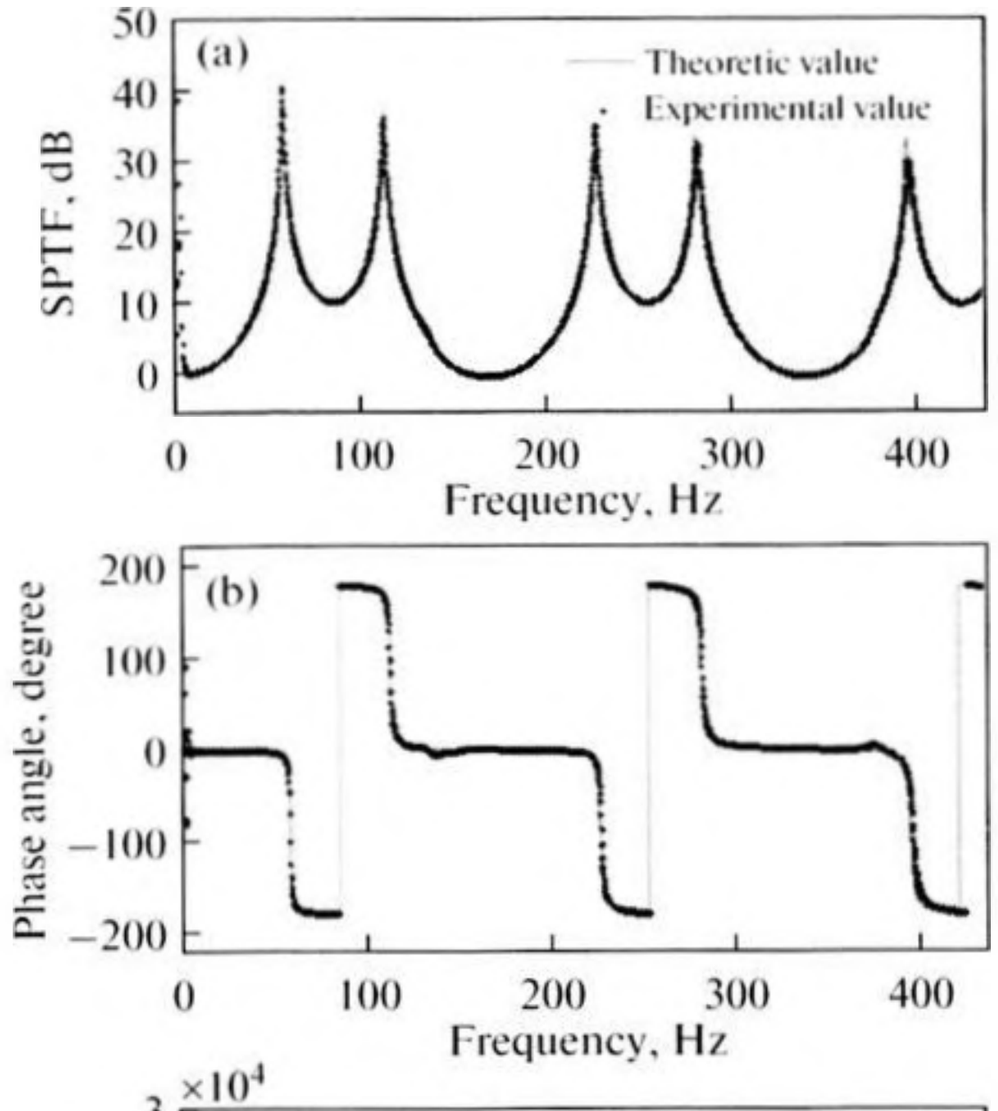


**Fig. 6.** Two-step resonator.

If attenuation is neglected, with boundary condition $v_0 = 0$, Eq. (8) can give the following resonance condition [7]

$$\tan(kl_1)\tan(kl_2) = d_1^2/d_2^2. \quad (9)$$

The resonance condition Eq. (9) is transcendental and the same as that figured out by the analytic methods [1, 19]. The frequencies corresponding to $k$ in Eq. (9) are the resonance frequencies and can be worked out numerically with Eq. (9).

Using Eq. (8), the numerical solutions of resonance frequency, phase angle and radiation impedance were shown in Fig. 6. The experimental results of the first two, resonance frequency and phase angle, were shown in Fig. 6 at the same time. Obviously, the numerical solutions are in excellent agreement with the experimental results. In contrast to those of the one-step resonator, the resonance frequencies of the two-step resonator do not distribute evenly in frequency domain and the SPTF of valley resonance frequencies do not always approach zero any more. The two-step resonator has a nonequidistant resonance frequency spectrum, and the length of the two-step resonator is neither equal to the odd times nor the even multiples of half-wavelength at the resonance frequencies. Nevertheless, the absolute values of phase angle of the peak resonance frequencies are still about 90°, and meanwhile those of the valley resonance frequencies are about 0° or 180°.

Dimensions of nos. 1 to 5 sub-tube

| No. | Wall thickness, mm | Length, mm | Inner diameter, mm | Cut-off frequency, 1 atm, 20°C, Hz |
|---|---|---|---|---|
| 1 | 10 | 1009 | 89 | 2261 |
| 2 | 10 | 1001 | 49 | 4107 |
| 3 | 10 | 1003 | 24 | 8385 |
| 4 | 5 | 1001 | 15 | 13416 |
| 5 | 7 | 1002 | 8 | 25155 |

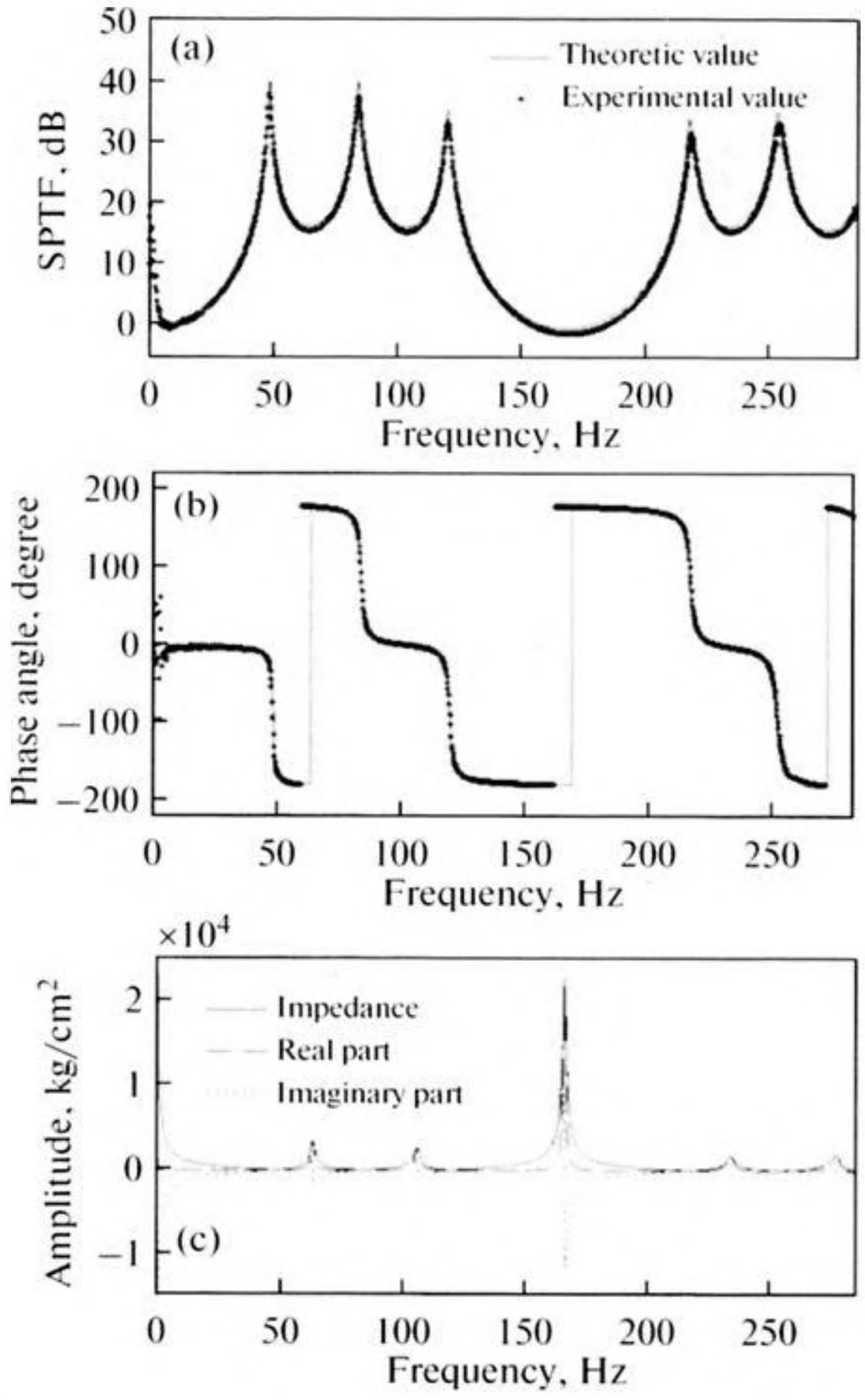


**Fig. 7.** Three-step resonator.

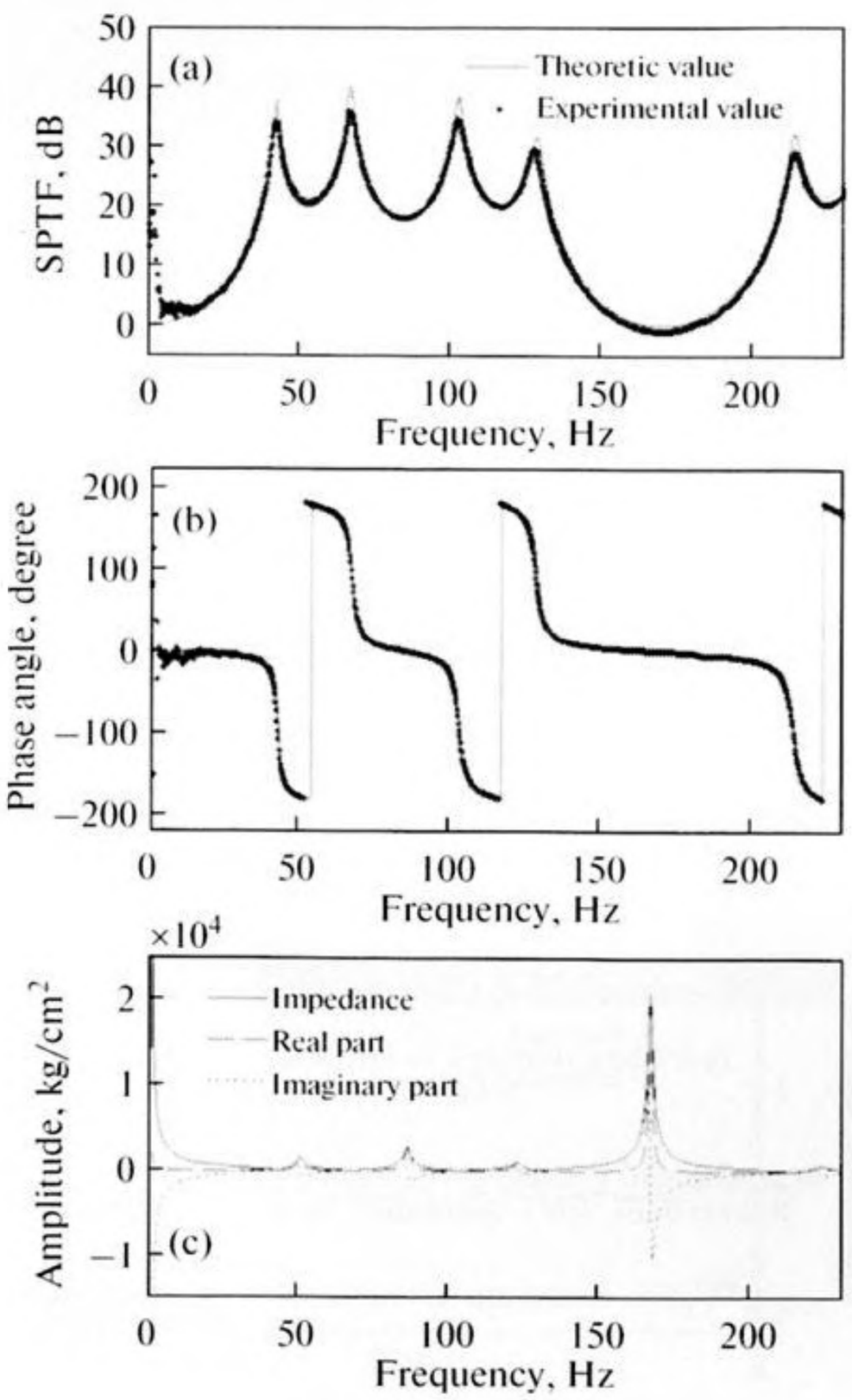


**Fig. 8.** Four-step resonator.

Additionally, the radiation impedances of the valley resonance frequencies do not decrease in sequence although all the radiation impedances of the peak resonance frequencies are still very low. The maximum of radiation impedance appears at the second valley resonance frequency and approaches $3 \times 10^4$ kg/cm$^2$, then the SPTF of the resonance frequency is the minimum.

### *4.3. Multi-Step Acoustic Resonator*

Taking the transfer matrix of the one-step acoustic resonator as the starting point, the research of the two-step acoustic resonator has tentatively displayed the capacity of transfer matrix method in the study of stepped resonator. As the number of the sub-tubes of stepped resonator increases, compared with analytic method, the advantage of transfer matrix method would become more and more remarkable. In the case of multi-step acoustic resonators, transfer matrixes can be worked out readily according to Eq. (6) and the boundary conditions of all output ports are $v_0 = 0$ as above.

As for the three kinds of multi-step resonators, namely the three-step resonator, the four-step resonator and the five-step resonator, besides the numerical solutions of radiation impedance, both the experimental results and the numerical solutions of resonance frequency and phase angle were shown in Figs. 7–9 as well. Unlike the one-step acoustic resonator, all the three multi-step resonators work the same as the two-step acoustic resonator in terms of the acoustic properties. The resonance frequencies do distribute unevenly in frequency domain, i.e., the multi-step acoustic resonators likewise have the dissonant acoustic properties as the two-step acoustic resonator. Besides, for any of the multi-step resonators, the peak resonance frequencies appear in groups and every group is separated by a valley resonance frequency of which the SPTF approximates zero. The number of peaks in each group is equal to the number of sub-tubes of the multi-step resonator, because the lengths of each sub-tube are nearly the same.

Still like the two-step acoustic resonator, for each multi-step resonator, the absolute values of phase angle of the peak resonance frequencies are about 90°,

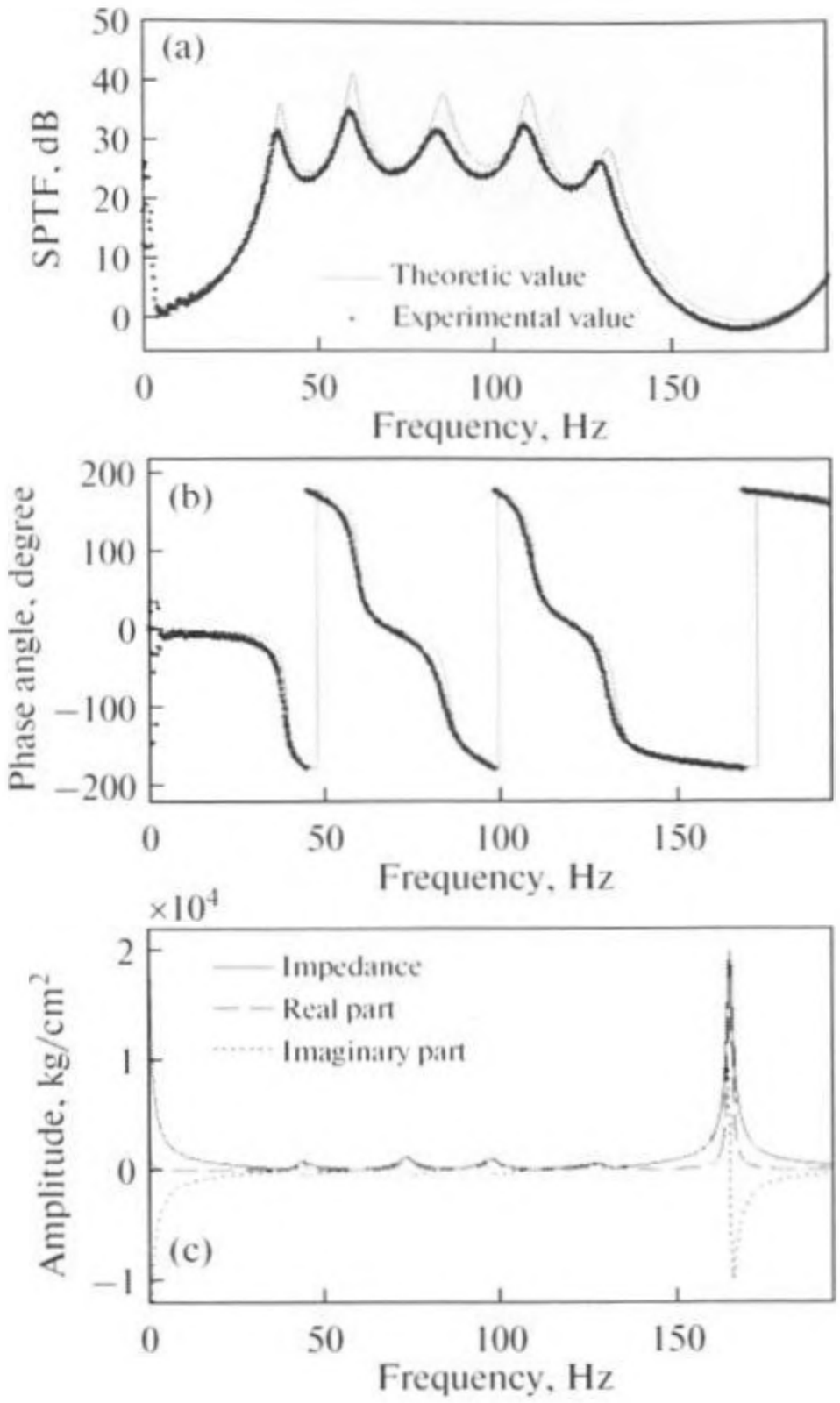


**Fig. 9.** Five-step resonator.

and meantime those of the valley resonance frequencies are about 0° or 180°. In addition, every valley resonance frequency corresponds to one peak of radiation impedance and the minimal valley of the resonance frequency corresponds to the maximum of radiation impedance. The maximum of radiation impedance of the three kinds of multi-step resonators decreases one by one from more than to less than $2 \times 10^4$ kg/cm$^2$.

## 5. CONCLUSIONS

Transfer matrix method was used to study the stepped acoustic resonators. Taking the transfer matrix of one-step acoustic resonator as a starting point, the transfer matrix of multi-step acoustic resonator could be developed conveniently from that of two-step acoustic resonator. With the help of numerical solution, transfer matrix method was more competent in comparison with analytic method to investigate the acoustic properties of stepped resonators, especially multi-step resonators. With the help of transfer matrix method, the resonance frequencies, the phase angles and the radiation impedances of the stepped acoustic resonators which were composed of one to five subtubes were studied theoretically and experimentally. The numerical solutions were in excellent agreement with the experimental results.

The one-step acoustic resonator had an equidistant resonance frequency spectrum in which the resonance frequencies distributed evenly in frequency domain while the resonance frequencies of the other stepped acoustic resonators were nonequidistant and appeared in groups. For all the stepped acoustic resonators, the valley resonance frequencies corresponded to the peaks of radiation impedance, and meanwhile, the peak resonance frequencies corresponded to the valleys of radiation impedance. Except the one-step acoustic resonator, the maximum of radiation impedance corresponded to the minimal valley of resonance frequency for any other stepped acoustic resonators. In addition, the absolute values of phase angle of the peak resonance frequencies were about 90°, and those of the valley resonance frequencies were about 0° or 180°.

The research was supported by the National Natural Science Foundation of China (Grant no. 11364017).

## REFERENCES

1. L. L. Beranek, *Acoustical Measurements* (Wiley, New York, 1998).
2. R. Ladbury, Phys. Today **51**, 23 (1998).
3. C. C. Lawrenson, B. Lipkens, T. S. Lucas, D. K. Perkins, and T. W. van Doren, J. Acoust. Soc. Am. **104**, 623 (1998).
4. Q. Min, Q. Y. Zhang, J. J. Tian, Q. B. Wang, and W. Q. He, Phys. Lett. A **377**, 99 (2012).
5. Q. Min, Y. Yin. X. D. Li and K. Liu, Acta Acoustica **30**, 409 (2011).
6. Q. Min, F. Peng, Y. Yin, and K. Liu, Acta Acoustica **29**, 321 (2010).
7. Q. Min and K. Liu, Acta Phys. Sin. **60**, 024301 (2011) [in Chinese].
8. D. F. Gaitan and A. A. Atchley, J. Acoust. Soc. Am. **93**, 2489 (1993).
9. Y. A. Ilinskii, B. Lipkens, T. S. Lucas, T. W. van Doren, and E. A. Zabolotskaya, J. Acoust. Soc. Am. **104**, 2664 (1998).
10. M. Bernard, Am. J. Phys. **64**, 745 (1996).
11. B. Denardo and M. Bernard, Am. J. Phys. **62**, 315 (1994).
12. V. Gibiat, A. Barjau, K. Casto, and E. B. Chazaud, Phys. Rev. E **67**, 066609 (2003).
13. M. L. Munjal, *Acoustics of Ducts and Mufflers with Application to Exhaust and Ventilation System Design* (Wiley, New York, 1987).
14. B. H. Song and J. S. Bolton, J. Acoust. Soc. Am. **107**, 1131 (2000).
15. I. S. Makarov, Acoust. Phys. **57**, 709 (2011).
16. V. F. Kovalev and O. V. Rudenko, Acoust. Phys. **58**, 269 (2012).
17. A. D. Pierce, *Acoustics: An Introduction to Its Physical Principles and Applications* (Melville, New York, 1989).
18. S. A. Nazarov, Acoust. Phys. **58**, 633 (2012).
19. B. J. Andersen and O. G. Symko, J. Acoust. Soc. Am. **125**, 787 (2009).